THE JOURNAL OF PHYSICAL CHEMISTRY Letters

pubs.acs.org/JPCL Letter

Size-Dependent Pressure-Response of the Photoluminescence of $CsPbBr_3$ Nanocrystals

J. Curtis Beimborn II, Luke R. Walther, Kenneth D. Wilson, and J. Mathias Weber*

Cite This: *J. Phys. Chem. Lett.* 2020, 11, 1975−1980 Read Online

ACCESS | Metrics & More | Article Recommendations | Supporting Information

ABSTRACT: We report the size-dependent pressure response for $CsPbBr_3$ perovskite nanocrystals in the size range 5.7−10.9 nm using photoluminescence spectroscopy in a diamond anvil cell. As the nanocrystal size decreases below ca. 7.5 nm, we observe a decrease in the transition pressure at which there is a change in the mode of deformation concomitant with an isostructural phase transition. We hypothesize that surface fluctuations regarding the tilt and distortion of surface $PbBr_6$ octahedra facilitate the change in the mode of deformation and phase transition at lower pressures for smaller nanocrystals.

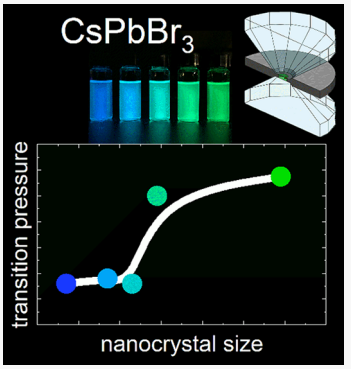

Metal halide perovskite nanocrystals (NCs) have attracted much attention in recent years for their unique electronic and optical properties as well as for their potential applications.[1−6] For example, perovskites have been used to make increasingly efficient solar cells, now surpassing 20%,[7,8] and the high surface defect tolerance of perovskite NCs allows photoluminescence (PL) quantum yields up to 90% without any surface modification,[9] reaching 100% with only minor postsynthetic treatment.[10,11]

Similar to other semiconductor NCs, the optical properties of perovskite NCs such as absorption and PL spectra depend on their size, changing significantly when the diameter or edge length is less than or equal to the material's bulk Bohr exciton diameter.[9,12−17] As the NC size decreases, the energy gap of the excitonic states is shifted to higher energies, blue-shifting their absorption and PL spectra. Along with changes to the band gap energy, other electronic properties such as recombination rates,[18] biexciton behavior,[19] and Stokes shifts[20,21] change as a function of NC size as well.

In addition to optical and electronic characteristics, thermodynamic and structural properties can also change as a function of NC size. As NC size decreases, the surface-to-volume ratio increases, altering the phase transition pressures of NCs. For example, the surface energy at constant pressure relaxes in the liquid phase relative to the solid phase, allowing melting at lower temperatures for smaller sizes, as the contribution of the surface energy to the overall internal energy of the NC grows.[22] Similarly, for many NC systems that have been studied so far, it has been shown that the pressure at which the NCs undergo a solid−solid phase transition (at constant temperature) increases as size decreases.[23−25] In most cases, particles converted from ambient phases to higher-pressure phases have higher index surfaces and therefore increased surface energy.[26] As a consequence, it usually takes greater pressure to force smaller NCs into the high-pressure phase.

Interestingly, many metal halide perovskite NC systems undergo an isostructural solid−solid phase transition from their ambient orthorhombic perovskite phase (γ-phase) to a second orthorhombic perovskite phase (not to be confused with the nonperovskite orthorhombic structure) under hydrostatic pressure.[27−31] This change manifests itself in a change in the mode of deformation as pressure increases further. Since the associated structural transition does not involve a change in surface indices, it is not at all clear a priori whether such pressure-induced phase changes follow a similar size dependence as in other materials, or whether metal halide perovskites display a qualitatively different behavior.

Detailed size dependent studies of perovskite nanocrystals are necessary to understand their properties and to optimize their performance in devices.[19,20,32−35] Recent improvements in methods for synthesizing NCs with higher stability and narrower size distributions[11,17,36,37] allow such experiments for $CsPbBr_3$ NCs. While some work in the literature has reported size dependent structural and optical properties,[19,32,33,38] there has been no study on the size dependence of their pressure

Received: January 16, 2020
Accepted: February 17, 2020
Published: February 17, 2020

https://dx.doi.org/10.1021/acs.jpclett.0c00174
J. Phys. Chem. Lett. 2020, 11, 1975−1980

response so far. The present work represents the first report on the pressure response of $CsPbBr_3$ NCs as a function of NC size. By applying high hydrostatic pressure to five NC samples of varying sizes with narrow size distributions (see Supporting Information for synthesis and characterization), we found that the PL pressure response of $CsPbBr_3$ NCs has a clear size dependence, deviating for the smallest NCs (below ca. 7.5 nm edge length) from that of the bulk behavior. More importantly, the observed behavior qualitatively differs from that of most other NC systems.[28,39]

Before addressing the PL pressure response in detail, it is necessary to discuss the structures of $CsPbBr_3$ NCs. When cesium lead halide perovskite NCs were first synthesized, there was disagreement in the literature over their crystal structure at ambient temperature and pressure.[9,40,41] Even in the most recent literature, some ambiguity remains as NCs with about 10 nm edge length can have a mixture of crystal structures at room temperature and ambient pressure. Atomically resolved high resolution transmission electron microscopy (HRTEM) of $CsPbBr_3$ NCs by Brennen et al. revealed that NCs with 5 nm edge size were entirely cubic in crystal structure, even though larger NCs were at least partially orthorhombic.[42] For 5 nm nanocrystals (and up to at least 6.5 nm), X-ray diffraction (XRD) patterns suffer from Scherrer broadening that made it impossible to unambiguously distinguish cubic from orthorhombic based on XRD alone.[33,43] Further, there is evidence of the coexistence of tetragonal and orthorhombic crystal structures in $CsPbBr_3$ NCs at liquid helium temperature, even though the orthorhombic to tetragonal phase transition is at 88 °C in bulk $CsPbBr_3$.[43,44] Similar behavior has been observed in oxide perovskites, where the structure of crystalline domains can vary, even in nanocrystalline samples. For example, $BaTiO_3$ NCs have a cubic "shell" surrounding a tetragonal "core."[45]

We analyzed our samples by XRD (Figure 1) at ambient temperature and pressure. For sizes ≤8 nm, the broadening due to overlap of the large number of diffraction features and Scherrer broadening make it impossible to make a conclusive structural assignment. However, we do observe diffraction features for $22° \leq 2\theta \leq 30°$ that suggest the γ perovskite crystal structure for all of our samples. The main difference between the cubic α-phase and the orthorhombic γ-phase is the symmetry reducing tilt of the $PbBr_6$ octahedra. In $CsPbI_3$ nanocrystals, the crystals adopt the γ-phase for all sizes that have been studied, although the smallest nanocrystals exhibit less of an octahedral tilt than the larger nanocrystals, which decreases the deviation from a cubic structure.[32] Taking our data and the recent results by Luther and co-workers on $CsPbI_3$ NCs into account, we assume that the $CsPbBr_3$ NC in the present work are orthorhombic for all sizes, even though the smallest sizes may experience less of an octahedral tilt than the larger sizes as was observed in $CsPbI_3$ NCs.[32,40−42] While this may seem to contradict the HRTEM results mentioned above, HRTEM is biased toward the structure of the surface, which could potentially exhibit even less octahedral tilt (resulting in an essentially cubic character) due to the high surface tension.[32,45]

Phase changes in metal halide perovskites can be studied by monitoring the PL spectrum of a NC sample as a function of pressure and temperature.[27,28,33] While in situ XRD is in most circumstances the cleanest way to determine the pressure dependent phase behavior of a material, Scherrer broadening for small sizes makes differentiating cubic from orthorhombic

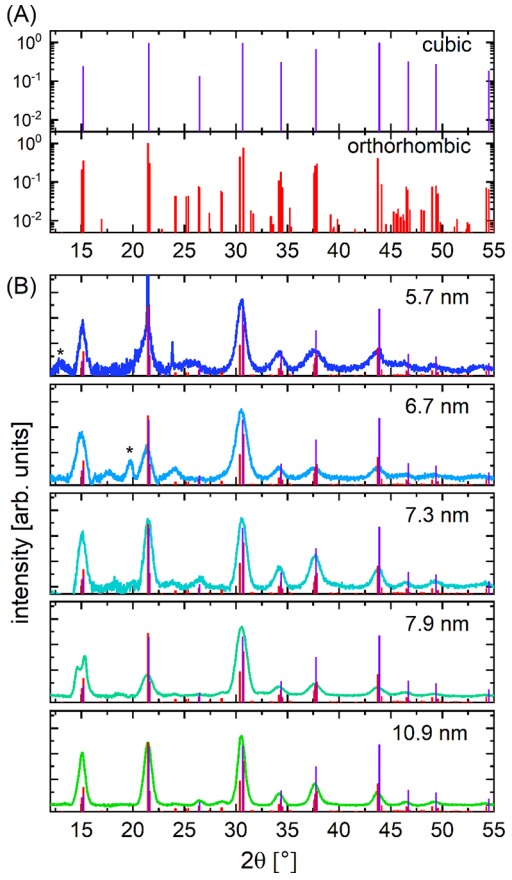

Figure 1. XRD Analysis of all nanocrystal samples used in our experiments. (A) Simulations for cubic and orthorhombic structures as a semilogarithmic plot to accentuate the low-intensity reflections. The red lines represent the orthorhombic perovskite pattern,[46] and the violet lines are for the cubic perovskite crystal structure.[47] (B) Comparison of experimental XRD data with the simulated patterns (linear scale). Peaks marked with an asterisk (appearing in some of the samples, most clearly for 5.7 and 6.7 nm edge length) are due to residual precursor material.

phases impossible,[32,43,44] as mentioned above, rendering optical approaches the best strategy in many cases. As a simple, phenomenological description of the pressure response, the pressure dependent change of the PL peak energy from ambient can be written as

$$\Delta E(p) = E(p_0) + \alpha(p)\cdot p \quad (1)$$

where α is a (pressure dependent) pressure coefficient encoding the shift of the PL peak. For various lead halide perovskites, a transition pressure has been shown to exist, where the response of their electronic structure to further pressure increase changes from a red shift to a blue-shift, i.e., where $\alpha(p)$ changes its sign.[27−29,39,48] This sign change can be explained by the orbital contributions to the band structure and by the change in the mode of deformation at the transition pressure.

In lead halide perovskites, the density of states at the valence band maximum (VBM) consists of Pb 6*s* and halide *p* orbitals with antibonding interaction between the two.[49−51] The conduction band minimum (CBM) is largely formed from Pb 6*p* orbitals and halide valence *p* orbitals with nonbonding interactions between them.[49−51] As pressure is applied to the perovskite crystal lattice, the mode of deformation at low

https://dx.doi.org/10.1021/acs.jpclett.0c00174
J. Phys. Chem. Lett. 2020, 11, 1975−1980

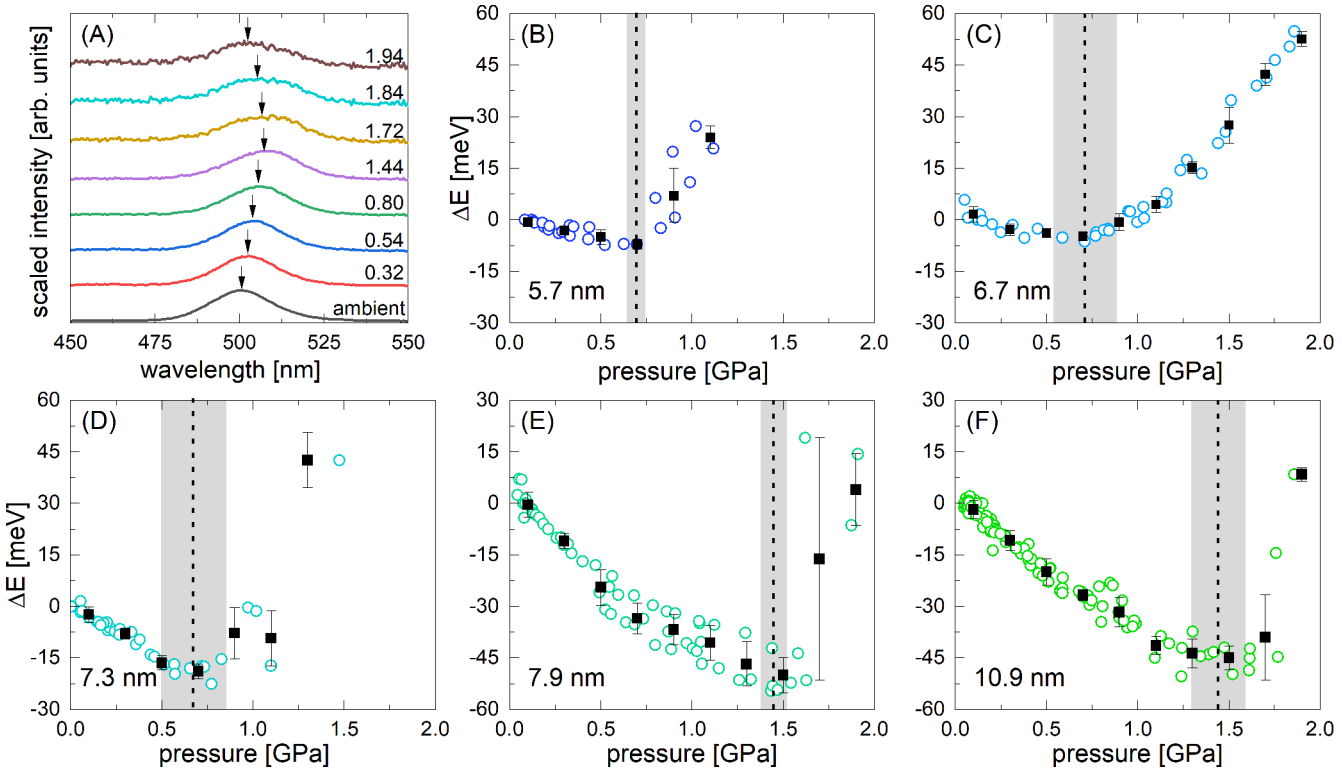

Figure 2. PL pressure response of NC samples studied in the present work. (A) PL spectra of the 7.9 nm sample as a function of pressure as an example for data from a typical high-pressure run (see Supporting Information for examples for all NC sizes). Arrows indicate the peak center from a single Lorentzian peak fit. (B–F) The difference in the PL peak energy from ambient conditions, ΔE, as a function of pressure. Open circles are raw data coming from at least two high pressure runs for each size, and black squares are the mean ΔE binned in pressure intervals of 0.2 GPa. The transition pressure is marked with vertical dotted lines with the uncertainty shaded in gray. The uncertainty in pressure for each data point is ±75 MPa.

pressures is characterized by isotropic compression of the PbX_6 octahedra, forcing greater overlap of the antibonding configuration of the Pb 6*s* and halide valence *p* orbitals.[3,50,52] The compression of the octahedra therefore destabilizes the VBM while leaving the CBM largely unaffected. This causes a decrease of the band gap energy that manifests itself as a red-shift of the PL peak.

At the transition pressure, this mode of deformation is no longer the softest, and the mode of deformation changes concomitant with the aforementioned isostructural phase transition.[30] Under continued pressure increase, instead of further octahedral compression, the octahedra begin to change the tilt angle relative to one another and distort, but they preserve the overall orthorhombic crystal symmetry in $CsPbBr_3$ and $CsPbI_3$ NCs.[27,40,41] This octahedral tilting and deformation diminishes the Pb character of the CBM and with it the stabilization of the CBM afforded by the spin orbit coupling in the Pb atoms.[49,53] Consequently, the CBM energy increases, while the VBM is mostly unaffected, which results in a blue-shift of the PL spectrum. This change in the sign of the pressure coefficient is a direct result of the change in the mode of deformation of the crystal lattice and the isostructural phase transition, so it can be used to track this structural change without using in situ X-ray diffraction measurements. This approach has been used from the earliest experiments on the pressure response of semiconductor NCs[54] to monitor phase change behavior in high-pressure experiments and has more recently also been employed for perovskite NCs in both high-pressure and temperature dependent experiments.[27,28,33]

The transition pressure and the pressure coefficients α for each NC size were found by pressurizing our NC samples in a diamond anvil cell while tracking the PL peak energy (Figure 2, see Supporting Information for experimental details). The transition pressure remains approximately constant with decreasing NC size for NCs above 7.5 nm, decreases for sizes around 7.5 nm edge length, and remains at a constant value or the smallest sizes studied here (Figure 3). For the largest NC samples, the transition pressure is slightly higher

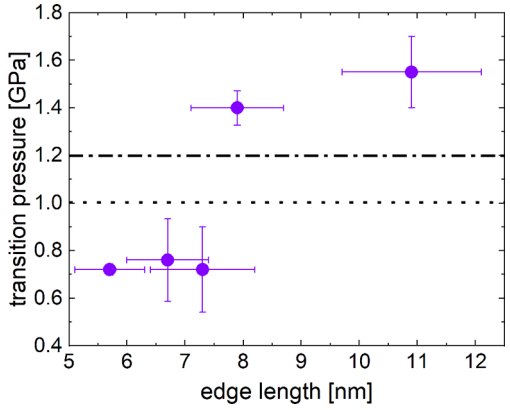

Figure 3. Transition pressure at which the PL turns from a red-shift to a blue-shift as a function of NC size. This is compared to the transition pressure in bulk $CsPbBr_3$ (dotted line) and the corresponding value reported in Xiao et al.[28] for 11.7 nm $CsPbBr_3$ NCs (dash-dotted line).

https://dx.doi.org/10.1021/acs.jpclett.0c00174
J. Phys. Chem. Lett. 2020, 11, 1975–1980

than in bulk samples. Finally, the magnitude of the initial pressure coefficient α, which is defined as $\alpha = dE/dp$, is relatively constant and close to the reported bulk value for NCs with edge lengths above 7.5 nm, then decreases in magnitude for edge lengths below 7 nm (Figure 4). We will discuss these

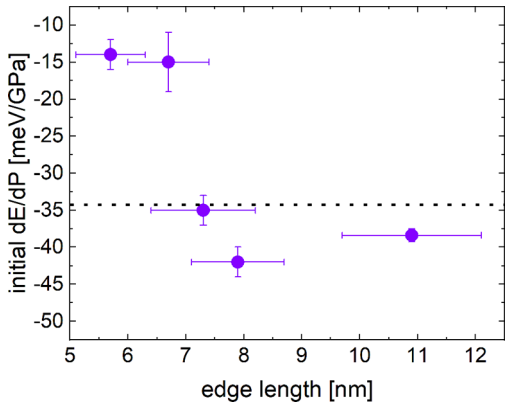

Figure 4. Magnitude of the initial pressure coefficient as a function of NC size. The dotted line represents the bulk pressure coefficient reported in Zhang et al.[60] It is worth noting that Xiao et al.[28] report a pressure coefficient of −91 meV/GPa for 11.7 nm $CsPbBr_3$ NCs. However, this drastic red-shift is likely due to sintering of NCs into bulk-like material as has been shown to occur in concentrated $CsPbBr_3$ NC samples under pressure.[61]

phenomena by taking into account the surface-to-volume ratio, together with the fact that solid−solid phase transitions in NCs occur simultaneously across the NC.[23,24,26,55−58]

In contrast to other NC materials, perovskite NCs undergo a change in the mode of deformation and in the tilting angle and distortion of the PbX_6 octahedra at their isostructural phase transition point, but they do not change the lattice indices of their facets.[27−29] Therefore, there is no significant surface rearrangement. This implies that there is not a large penalty in the surface energy, so the change in the overall internal energy of the NCs at the transition does not increase drastically as the NC size decreases.

Figure 3 shows the size dependence of the pressure at which this change in the mode of deformation occurs. For the largest sizes studied here, the transition pressure slowly diminishes as the NC size decreases. For nanocrystal samples around 7.5 nm edge length, there is a stronger decrease in the transition pressure, which then remains constant as NC size decreases further. The observed behavior could be due to multiple factors.

It is well-known that NCs undergo phase transitions starting from one nucleation site.[23,26,54,56−58] For the smallest sizes, the fluctuation length scale that can cause an isostructural phase transition involving a different octahedral tilt can be shorter than for the larger NCs. Low energy Raman spectroscopy results on $CsPbBr_3$ have shown that local polar fluctuations at room temperature cause the Cs^+ ion to be displaced off center, inducing tilting in the octahedra.[59] With a higher surface-to-volume ratio, surface fluctuations that tilt the octahedra on small NCs may be more likely to cause a coherent phase transition than in larger NCs, leading to a lower transition pressure.

The transition pressure for NCs with sizes from 5.7 to 7.3 nm edge length remains constant around 0.75 GPa. The change in the transition pressure may be an indication that as the size is decreased below 7.5 nm, the nanocrystals adopt a crystal structure with less octahedral tilt at ambient pressure, closer to the cubic perovskite structure. As the crystal structure is compressed under pressure with less initial tilt, it may begin to deform by tilting/distorting the octahedra at a lower pressure than crystals that are already starting with tilted octahedra at ambient conditions. This would initiate the decrease of Pb 6*p* character in the CBM at a lower pressure, indicated by a change in the sign of α. Our PL measurements do not provide direct information about octahedral tilt or distortion at any given pressure, but they can tell us about a change in octahedral tilt or distortion from one pressure to the next, because an increase in the tilt/distortion causes destabilization of the CBM. The point at which the effect of the destabilization of the CBM becomes greater than the destabilization of the VBM (due to isotropic octahedral compression), causing a blue-shift of the band gap energy, may be significantly lower for smaller perovskite NCs.

In addition to having a lower transition pressure, NCs below 7.5 nm edge length also show a smaller magnitude of the initial pressure coefficient for the isotropic compression phase (Figure 4). As nanocrystal size decreases, the lattice constants increase due to higher surface tension,[32] and the overlap of the Pb 6*s* and Br 4*p* orbitals is therefore initially less than for larger NCs with smaller lattice constants. As the crystal is compressed, the increase in overlap does not have as pronounced an effect as it does for larger NCs with greater initial orbital overlap. If all the nanocrystals continued to deform in this mode only, we would expect to see an increase in the magnitude of the pressure coefficient with increasing pressure. However, the destabilization of the CBM due to tilting/distortion of the octahedra competes with and eventually surpasses the effects of compression, likely before we can observe the pressure coefficient becoming more negative.

In summary, we have probed the isostructural phase transition pressures and PL pressure coefficients for a range of sizes of $CsPbBr_3$ NCs using PL spectroscopy. Contrary to NC systems whose pressure induced solid−solid phase transitions involve changing the crystal symmetry, we observed a reduction in the phase transition pressure as NC size decreases. We explain this observation by the fact that the lowest pressure phase transition in perovskite NCs does not lead to the formation of high index facets. Furthermore, the smaller size of the NCs means that the fluctuation length scale needed to cause a coherent transition is necessarily smaller than for the larger NCs. These two factors lead to the reduction of the transition pressure as NC size is decreased. Finally, the expansion of the lattice at ambient pressures as NC size decreases[32] can explain the observed size dependent reduction of the pressure coefficient.

■ ASSOCIATED CONTENT

Supporting Information

The Supporting Information is available free of charge at https://pubs.acs.org/doi/10.1021/acs.jpclett.0c00174.

Nanocrystal synthesis, photoluminescence measurements, TEM characterization, XRD characterization, and summary of high-pressure experimental details (PDF)

https://dx.doi.org/10.1021/acs.jpclett.0c00174
J. Phys. Chem. Lett. 2020, 11, 1975−1980

AUTHOR INFORMATION

Corresponding Author

J. Mathias Weber − *JILA and the Department of Chemistry, University of Colorado, Boulder, Colorado 80309-0440, United States;* orcid.org/0000-0002-5493-5886; Phone: (303) 492-7841; Email: weberjm@jila.colorado.edu

Authors

J. Curtis Beimborn II − *JILA and the Department of Chemistry, University of Colorado, Boulder, Colorado 80309-0440, United States*

Luke R. Walther − *JILA and the Department of Chemistry, University of Colorado, Boulder, Colorado 80309-0440, United States*

Kenneth D. Wilson − *JILA and the Department of Chemistry, University of Colorado, Boulder, Colorado 80309-0440, United States*

Complete contact information is available at: https://pubs.acs.org/10.1021/acs.jpclett.0c00174

Notes

The authors declare no competing financial interest.

ACKNOWLEDGMENTS

We thank Garry Morgan (University of Colorado Boulder) for TEM facility services. We gratefully acknowledge the National Science Foundation for support through the JILA AMO Physics Frontier Center under grant PHY-1734006.

REFERENCES

(1) Milstein, T. J.; Kroupa, D. M.; Gamelin, D. R. Picosecond Quantum Cutting Generates Photoluminescence Quantum Yields Over 100% in Ytterbium-Doped $CsPbCl_3$ Nanocrystals. *Nano Lett.* **2018**, *18*, 3792−3799.

(2) Fu, Y.; Zhu, H.; Chen, J.; Hautzinger, M. P.; Zhu, X. Y.; Jin, S. Metal Halide Perovskite Nanostructures for Optoelectronic Applications and the Study of Physical Properties. *Nat. Rev. Mater.* **2019**, *4*, 169−188.

(3) Manser, J. S.; Christians, J. A.; Kamat, P. V. Intriguing Optoelectronic Properties of Metal Halide Perovskites. *Chem. Rev.* **2016**, *116*, 12956−13008.

(4) Akkerman, Q. A.; Rainò, G.; Kovalenko, M. V.; Manna, L. Genesis, Challenges and Opportunities for Colloidal Lead Halide Perovskite Nanocrystals. *Nat. Mater.* **2018**, *17*, 394−405.

(5) Jena, A. K.; Kulkarni, A.; Miyasaka, T. Halide Perovskite Photovoltaics: Background, Status, and Future Prospects. *Chem. Rev.* **2019**, *119*, 3036−3103.

(6) Shamsi, J.; Urban, A. S.; Imran, M.; De Trizio, L.; Manna, L. Metal Halide Perovskite Nanocrystals: Synthesis, Post-Synthesis Modifications, and Their Optical Properties. *Chem. Rev.* **2019**, *119*, 3296−3348.

(7) Green, M. A.; Dunlop, E. D.; Hohl-Ebinger, J.; Yoshita, M.; Kopidakis, N.; Ho-Baillie, A. W. Y. Solar Cell Efficiency Tables (Version 55). *Prog. Photovoltaics* **2020**, *28*, 3−15.

(8) Jung, E. H.; Jeon, N. J.; Park, E. Y.; Moon, C. S.; Shin, T. J.; Yang, T.-Y.; Noh, J. H.; Seo, J. Efficient, Stable and Scalable Perovskite Solar Cells using Poly(3-Hexylthiophene). *Nature* **2019**, *567*, 511−515.

(9) Protesescu, L.; Yakunin, S.; Bodnarchuk, M. I.; Krieg, F.; Caputo, R.; Hendon, C. H.; Yang, R. X.; Walsh, A.; Kovalenko, M. V. Nanocrystals of Cesium Lead Halide Perovskites ($CsPbX_3$, X = Cl, Br, and I): Novel Optoelectronic Materials Showing Bright Emission with Wide Color Gamut. *Nano Lett.* **2015**, *15*, 3692−3696.

(10) Koscher, B. A.; Swabeck, J. K.; Bronstein, N. D.; Alivisatos, A. P. Essentially Trap-Free $CsPbBr_3$ Colloidal Nanocrystals by Postsynthetic Thiocyanate Surface Treatment. *J. Am. Chem. Soc.* **2017**, *139*, 6566−6569.

(11) Nenon, D. P.; Pressler, K.; Kang, J.; Koscher, B. A.; Olshansky, J. H.; Osowiecki, W. T.; Koc, M. A.; Wang, L.-W.; Alivisatos, A. P. Design Principles for Trap-Free $CsPbX_3$ Nanocrystals: Enumerating and Eliminating Surface Halide Vacancies with Softer Lewis Bases. *J. Am. Chem. Soc.* **2018**, *140*, 17760−17772.

(12) Rossetti, R.; Ellison, J. L.; Gibson, J. M.; Brus, L. E. Size Effects in the Excited Electronic States of Small Colloidal CdS Crystallites. *J. Chem. Phys.* **1984**, *80*, 4464−4469.

(13) Norris, D. J.; Bawendi, M. G. Measurement and Assignment of the Size-Dependent Optical Spectrum in CdSe Quantum Dots. *Phys. Rev. B: Condens. Matter Mater. Phys.* **1996**, *53*, 16338−16346.

(14) Brus, L. E. Electron−Electron and Electron-Hole Interactions in Small Semiconductor Crystallites: The Size Dependence of the Lowest Excited Electronic State. *J. Chem. Phys.* **1984**, *80*, 4403−4409.

(15) Wang, Y.; Herron, N. Nanometer-Sized Semiconductor Clusters: Materials Synthesis, Quantum Size Effects, and Photophysical Properties. *J. Phys. Chem.* **1991**, *95*, 525−532.

(16) Steigerwald, M. L.; Brus, L. E. Semiconductor Crystallites: a Class of Large Molecules. *Acc. Chem. Res.* **1990**, *23*, 183−188.

(17) Dong, Y.; Qiao, T.; Kim, D.; Parobek, D.; Rossi, D.; Son, D. H. Precise Control of Quantum Confinement in Cesium Lead Halide Perovskite Quantum Dots via Thermodynamic Equilibrium. *Nano Lett.* **2018**, *18*, 3716−3722.

(18) Cohn, A. W.; Schimpf, A. M.; Gunthardt, C. E.; Gamelin, D. R. Size-Dependent Trap-Assisted Auger Recombination in Semiconductor Nanocrystals. *Nano Lett.* **2013**, *13*, 1810−1815.

(19) Ashner, M. N.; Shulenberger, K. E.; Krieg, F.; Powers, E. R.; Kovalenko, M. V.; Bawendi, M. G.; Tisdale, W. A. Size-Dependent Biexciton Spectrum in $CsPbBr_3$ Perovskite Nanocrystals. *ACS Energy Lett.* **2019**, *4*, 2639−2645.

(20) Brennan, M. C.; Herr, J. E.; Nguyen-Beck, T. S.; Zinna, J.; Draguta, S.; Rouvimov, S.; Parkhill, J.; Kuno, M. Origin of the Size-Dependent Stokes Shift in $CsPbBr_3$ Perovskite Nanocrystals. *J. Am. Chem. Soc.* **2017**, *139*, 12201−12208.

(21) Liptay, T. J.; Marshall, L. F.; Rao, P. S.; Ram, R. J.; Bawendi, M. G. Anomalous Stokes Shift in CdSe Nanocrystals. *Phys. Rev. B: Condens. Matter Mater. Phys.* **2007**, *76*, 155314.

(22) Goldstein, A. N.; Echer, C. M.; Alivisatos, A. P. Melting in Semiconductor Nanocrystals. *Science* **1992**, *256*, 1425.

(23) Tolbert, S. H.; Alivisatos, A. P. High-Pressure Structural Transformations in Semiconductor Nanocrystals. *Annu. Rev. Phys. Chem.* **1995**, *46*, 595−626.

(24) Chen, C.-C.; Herhold, A. B.; Johnson, C. S.; Alivisatos, A. P. Size Dependence of Structural Metastability in Semiconductor Nanocrystals. *Science* **1997**, *276*, 398.

(25) Chen, Z.; Sun, C. Q.; Zhou, Y.; Ouyang, G. Size Dependence of the Pressure-Induced Phase Transition in Nanocrystals. *J. Phys. Chem. C* **2008**, *112*, 2423−2427.

(26) Herhold, A. B.; Tolbert, S. H.; Guzelian, A. A.; Alivisatos, A. P., A Comparison of Pressure-Induced Structural Transformations in CdSe, InP, and Si Nanocrystals. In *Fine Particles Science and Technology: From Micro to Nanoparticles*; Pelizzetti, E., Ed.; Springer Netherlands: Dordrecht, 1996; pp 331−342.

(27) Beimborn, J. C.; Hall, L. M. G.; Tongying, P.; Dukovic, G.; Weber, J. M. Pressure Response of Photoluminescence in Cesium Lead Iodide Perovskite Nanocrystals. *J. Phys. Chem. C* **2018**, *122*, 11024−11030.

(28) Xiao, G.; Cao, Y.; Qi, G.; Wang, L.; Liu, C.; Ma, Z.; Yang, X.; Sui, Y.; Zheng, W.; Zou, B. Pressure Effects on Structure and Optical Properties in Cesium Lead Bromide Perovskite Nanocrystals. *J. Am. Chem. Soc.* **2017**, *139*, 10087−10094.

(29) Cao, Y.; Qi, G.; Liu, C.; Wang, L.; Ma, Z.; Wang, K.; Du, F.; Xiao, G.; Zou, B. Pressure-Tailored Band Gap Engineering and Structure Evolution of Cubic Cesium Lead Iodide Perovskite Nanocrystals. *J. Phys. Chem. C* **2018**, *122*, 9332−9338.

(30) Kincaid, J. M.; Stell, G.; Goldmark, E. Isostructural Phase Transitions Due to Core Collapse. II. A Three-Dimensional Model

with a Solid−Solid Critical Point. *J. Chem. Phys.* **1976**, *65*, 2172−2179.
(31) Li, M.; Liu, T.; Wang, Y.; Yang, W.; Lü, X. Pressure Responses of Halide Perovskites With Various Compositions, Dimensionalities, and Morphologies. *Matter Radiat. at Extremes* **2020**, *5*, No. 018201.
(32) Zhao, Q.; Hazarika, A.; Schelhas, L. T.; Liu, J.; Gaulding, E. A.; Li, G.; Zhang, M.; Toney, M. F.; Sercel, P. C.; Luther, J. M. Size-Dependent Lattice Structure and Confinement Properties in $CsPbI_3$ Perovskite Nanocrystals: Negative Surface Energy for Stabilization. *ACS Energy Lett.* **2020**, *5*, 238−247.
(33) Liu, L.; Zhao, R.; Xiao, C.; Zhang, F.; Pevere, F.; Shi, K.; Huang, H.; Zhong, H.; Sychugov, I. Size-Dependent Phase Transition in Perovskite Nanocrystals. *J. Phys. Chem. Lett.* **2019**, *10*, 5451−5457.
(34) Butkus, J.; Vashishtha, P.; Chen, K.; Gallaher, J. K.; Prasad, S. K. K.; Metin, D. Z.; Laufersky, G.; Gaston, N.; Halpert, J. E.; Hodgkiss, J. M. The Evolution of Quantum Confinement in $CsPbBr_3$ Perovskite Nanocrystals. *Chem. Mater.* **2017**, *29*, 3644−3652.
(35) Scheidt, R. A.; Atwell, C.; Kamat, P. V. Tracking Transformative Transitions: From $CsPbBr_3$ Nanocrystals to Bulk Perovskite Films. *ACS Mater. Lett.* **2019**, *1*, 8−13.
(36) Dutta, A.; Dutta, S. K.; Das Adhikari, S.; Pradhan, N. Tuning the Size of $CsPbBr_3$ Nanocrystals: All at One Constant Temperature. *ACS Energy Lett.* **2018**, *3*, 329−334.
(37) Yoo, D.; Woo, J. Y.; Kim, Y.; Kim, S. W.; Wei, S.-H.; Jeong, S.; Kim, Y.-H. Origin of the Stability and Transition from Anionic to Cationic Surface Ligand Passivation of All-Inorganic Cesium Lead Halide Perovskite Nanocrystals. *J. Phys. Chem. Lett.* **2020**, *11*, 652−658.
(38) Naghadeh, S. B.; Sarang, S.; Brewer, A.; Allen, A. L.; Chiu, Y.-H.; Hsu, Y.-J.; Wu, J.-Y.; Ghosh, S.; Zhang, J. Z. Size and Temperature Dependence of Photoluminescence of Hybrid Perovskite Nanocrystals. *J. Chem. Phys.* **2019**, *151*, 154705.
(39) Wang, L.; Wang, K.; Xiao, G.; Zeng, Q.; Zou, B. Pressure-Induced Structural Evolution and Band Gap Shifts of Organometal Halide Perovskite-Based Methylammonium Lead Chloride. *J. Phys. Chem. Lett.* **2016**, *7*, 5273−5279.
(40) Cottingham, P.; Brutchey, R. L. On The Crystal Structure of Colloidally Prepared $CsPbBr_3$ Quantum Dots. *Chem. Commun.* **2016**, *52*, 5246−5249.
(41) Bertolotti, F.; Protesescu, L.; Kovalenko, M. V.; Yakunin, S.; Cervellino, A.; Billinge, S. J. L.; Terban, M. W.; Pedersen, J. S.; Masciocchi, N.; Guagliardi, A. Coherent Nanotwins and Dynamic Disorder in Cesium Lead Halide Perovskite Nanocrystals. *ACS Nano* **2017**, *11*, 3819−3831.
(42) Brennan, M. C.; Kuno, M.; Rouvimov, S. Crystal Structure of Individual $CsPbBr_3$ Perovskite Nanocubes. *Inorg. Chem.* **2019**, *58*, 1555−1560.
(43) Fu, M.; Tamarat, P.; Huang, H.; Even, J.; Rogach, A. L.; Lounis, B. Neutral and Charged Exciton Fine Structure in Single Lead Halide Perovskite Nanocrystals Revealed by Magneto-Optical Spectroscopy. *Nano Lett.* **2017**, *17*, 2895−2901.
(44) Ramade, J.; Andriambariarijaona, L. M.; Steinmetz, V.; Goubet, N.; Legrand, L.; Barisien, T.; Bernardot, F.; Testelin, C.; Lhuillier, E.; Bramati, A.; et al. Fine Structure of Excitons and Electron−Hole Exchange Energy in Polymorphic $CsPbBr_3$ Single Nanocrystals. *Nanoscale* **2018**, *10*, 6393−6401.
(45) Aoyagi, S.; Kuroiwa, Y.; Sawada, A.; Kawaji, H.; Atake, T. Size Effect on Crystal Structure and Chemical Bonding Nature in $BaTiO_3$ Nanopowder. *J. Therm. Anal. Calorim.* **2005**, *81*, 627−630.
(46) Stoumpos, C. C.; Malliakas, C. D.; Peters, J. A.; Liu, Z.; Sebastian, M.; Im, J.; Chasapis, T. C.; Wibowo, A. C.; Chung, D. Y.; Freeman, A. J.; et al. Crystal Growth of the Perovskite Semiconductor CsPbBr3: A New Material for High-Energy Radiation Detection. *Cryst. Growth Des.* **2013**, *13*, 2722−2727.
(47) Rodová, M.; Brožek, J.; Knížek, K.; Nitsch, K. Phase Transitions in Ternary Caesium Lead Bromide. *J. Therm. Anal. Calorim.* **2003**, *71*, 667−673.
(48) Li, Q.; Li, S.; Wang, K.; Quan, Z.; Meng, Y.; Zou, B. High-Pressure Study of Perovskite-Like Organometal Halide: Band-Gap Narrowing and Structural Evolution of $[NH_3\text{-}(CH_2)_4\text{-}NH_3]CuCl_4$. *J. Phys. Chem. Lett.* **2017**, *8*, 500−506.
(49) Lee, J.-H.; Bristowe, N. C.; Lee, J. H.; Lee, S.-H.; Bristowe, P. D.; Cheetham, A. K.; Jang, H. M. Resolving the Physical Origin of Octahedral Tilting in Halide Perovskites. *Chem. Mater.* **2016**, *28*, 4259−4266.
(50) Prasanna, R.; Gold-Parker, A.; Leijtens, T.; Conings, B.; Babayigit, A.; Boyen, H.-G.; Toney, M. F.; McGehee, M. D. Band Gap Tuning via Lattice Contraction and Octahedral Tilting in Perovskite Materials for Photovoltaics. *J. Am. Chem. Soc.* **2017**, *139*, 11117−11124.
(51) Garcia-Fernandez, P.; Aramburu, J. A.; Barriuso, M. T.; Moreno, M. Key Role of Covalent Bonding in Octahedral Tilting in Perovskites. *J. Phys. Chem. Lett.* **2010**, *1*, 647−651.
(52) Ghosh, D.; Aziz, A.; Dawson, J. A.; Walker, A. B.; Islam, M. S. Putting the Squeeze on Lead Iodide Perovskites: Pressure-Induced Effects To Tune Their Structural and Optoelectronic Behavior. *Chem. Mater.* **2019**, *31*, 4063−4071.
(53) Amat, A.; Mosconi, E.; Ronca, E.; Quarti, C.; Umari, P.; Nazeeruddin, M. K.; Gratzel, M.; De Angelis, F. Cation-Induced Band-Gap Tuning in Organohalide Perovskites: Interplay of Spin-Orbit Coupling and Octahedra Tilting. *Nano Lett.* **2014**, *14*, 3608−3616.
(54) Tolbert, S. H.; Alivisatos, A. P. Size Dependence of the Solid-Solid Phase Transition in CdSe Nanocrystals. *Z. Phys. D: At., Mol. Clusters* **1993**, *26*, 56−58.
(55) Brus, L. E.; Harkless, J. A. W.; Stillinger, F. H. Theoretical Metastability of Semiconductor Crystallites in High-Pressure Phases, with Application to β-Tin Structure Silicon. *J. Am. Chem. Soc.* **1996**, *118*, 4834−4838.
(56) Tolbert, S. H.; Alivisatos, A. P. The Wurtzite to Rock Salt Structural Transformation in CdSe Nanocrystals Under High Pressure. *J. Chem. Phys.* **1995**, *102*, 4642−4656.
(57) Tolbert, S. H.; Herhold, A. B.; Brus, L. E.; Alivisatos, A. P. Pressure-Induced Structural Transformations in Si Nanocrystals: Surface and Shape Effects. *Phys. Rev. Lett.* **1996**, *76*, 4384−4387.
(58) Grünwald, M.; Lutker, K.; Alivisatos, A. P.; Rabani, E.; Geissler, P. L. Metastability in Pressure-Induced Structural Transformations of CdSe/ZnS Core/Shell Nanocrystals. *Nano Lett.* **2013**, *13*, 1367−1372.
(59) Yaffe, O.; Guo, Y.; Tan, L. Z.; Egger, D. A.; Hull, T.; Stoumpos, C. C.; Zheng, F.; Heinz, T. F.; Kronik, L.; Kanatzidis, M. G.; et al. Local Polar Fluctuations in Lead Halide Perovskite Crystals. *Phys. Rev. Lett.* **2017**, *118*, 136001.
(60) Zhang, L.; Zeng, Q.; Wang, K. Pressure-Induced Structural and Optical Properties of Inorganic Halide Perovskite $CsPbBr_3$. *J. Phys. Chem. Lett.* **2017**, *8*, 3752−3758.
(61) Nagaoka, Y.; Hills-Kimball, K.; Tan, R.; Li, R.; Wang, Z.; Chen, O. Nanocube Superlattices of Cesium Lead Bromide Perovskites and Pressure-Induced Phase Transformations at Atomic and Mesoscale Levels. *Adv. Mater.* **2017**, *29*, 1606666.

https://dx.doi.org/10.1021/acs.jpclett.0c00174
J. Phys. Chem. Lett. 2020, 11, 1975−1980